Wayne State University

**COLLEGE OF
ENGINEERING**

to: CASI

NASA/CR-94- 206676

INTERIM
MN-44-CR
18 CiT.
047876

Final Report To:	National Aeronautics and Space Administration Lewis Research Center
Title:	Radiation Resistance Studies of Amorphous Silicon Alloy Photovoltaic Materials
Grant Number:	NASA Grant NAG 3-833
Reporting Period:	November 5, 1987 to March 31, 1994
Submitted By:	James R. Woodyard Associate Professor Department of Electrical and Computer Engineering (313) 577-3758
Signature and Date:	James R. Woodyard 12/23/97

ABSTRACT

The radiation resistance of commercial solar cells fabricated from hydrogenated amorphous silicon alloys was investigated. A number of different device structures were irradiated with 1.0 MeV protons. The cells were insensitive to proton fluences below 1E12 cm^2 The parameters of the irradiated cells were restored with annealing at 200 °C. The annealing time was dependent on proton fluence. Annealing devices for one hour restores cell parameters for fluences below 1E14 cm^2 fluences above 1E14 cm^2 require longer annealing times. A parametric fitting model was used to characterize current mechanisms observed in dark I-V measurements. The current mechanisms were explored with irradiation fluence, and voltage and light soaking times. The thermal generation current density and quality factor increased with proton fluence. Device simulation shows the degradation in cell characteristics may be explained by the reduction of the electric field in the intrinsic layer.

TABLE OF CONTENTS

INTRODUCTION

The goal of our research is to develop a model to predict EOL performance of thin-film solar cells in space environments. In order to achieve the goal we have irradiated and characterized a number of different thin-film solar cell device structures fabricated from hydrogenated amorphous silicon alloys (refs. 1-5). The radiation resistance of single, dual and triple junction cells has been determined for 1.0 MeV proton fluences in the 1E11 through 1E15 cm^{-2} range. Both substrate and superstrate cell structures obtained from three companies producing commercial modules have been investigated. The p-i-n layers in the cells are made up of hydrogenated amorphous silicon alloys deposited using plasma enhanced chemical vapor deposition; the details of cell structures have been reported in references one through five. Cells were characterized using light I-V, dark I-V and quantum efficiency measurements.

Six cell structures have been investigated by our group. The results of 1.0 MeV proton irradiation on cell normalized power density are shown in Figure 1. Measurements on single and triple-junction cells with superstrate structures are shown. The triple-junction cells had two band gaps. The i-layers of the top two junctions were a-Si:H with the same band gap; the i-layer of the bottom junction was a-Si,Ge:H with a lower band gap than the top two junctions. Tandem and single-junction cells with substrate structures are also shown in Figure 1; tandems with single and dual gaps were investigated as well as single-junction cells with
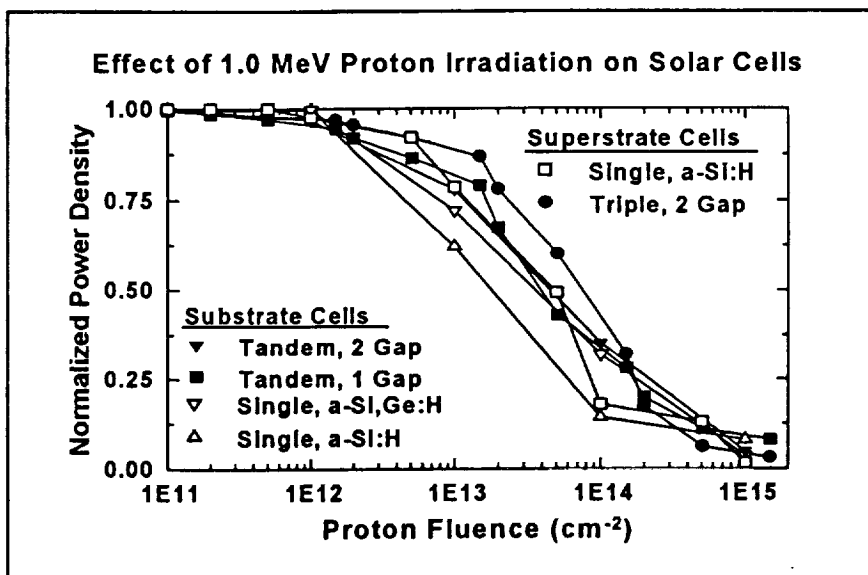
Figure 1. Plot comparing the effect of 1.0 MeV proton irradiation on the normalized power density of a-Si:H alloy based solar cells.

a-Si:H and a-Si,Ge:H i-layers. The cell efficiencies ranged between seven and eight percent under AM1.5 global irradiance; the radiation resistance of the cells has been reported in prior papers published by our group (refs. 1-5). Figure 1 shows 1.0 MeV proton irradiation degrades the normalized power density of all the cells by less than a few percent for fluences less than 1E12 cm^{-2} For fluences above 1E15 cm^{-2} the cell power degrades to less than 10% of the initial power. Reductions in the normalized power density in the 1E12 through 1E14 cm^{-2} proton fluence range depends on cell structure. Cells with triple junctions have the best radiation resistance, dual-junction cells are next and single-junction cells have the lowest radiation resistance. Single-junction cells with a-Si,Ge:H i-layers have better radiation resistance than cells with a-Si:H i-layers; it is not

clear whether the effect is due to the role of germanium in these cells or the differences in the thicknesses of the i-layers. The i-layers of the a-Si,Ge:H single-junction cells are thinner than the i-layers of the a-Si:H cells.

The effect of post-irradiation annealing at 200 °C on the normalized power density of twenty-one solar cells fabricated from hydrogenated amorphous silicon alloys is illustrated in Figure 2. The data are for single-junction cells with a superstrate structure and 500 nm i-layer thickness. Three cells were irradiated at each fluence; the power densities following irradiation are shown by the open squares. The average power density of three irradiated cells at each fluence is shown by the filled squares. The power densities following a two-hour anneal at 200 °C are shown by the open triangles with the averages represented by the filled triangles. Annealing the cells for one hour restores the normalized power density of cells irradiated with 1.0 MeV proton fluences less than 1E14 cm^{-2} fluences above 1E14 cm^{-2} require longer annealing times to restore the normalized power density. This is shown by the data in Figure 3. The average power density of the three single-junction cells irradiated with a fluence of 1.5E15 cm^{-2} recovers to 6.2 and 7.0 mW/cm^2 with 2.0 and 4.0 hours annealing,
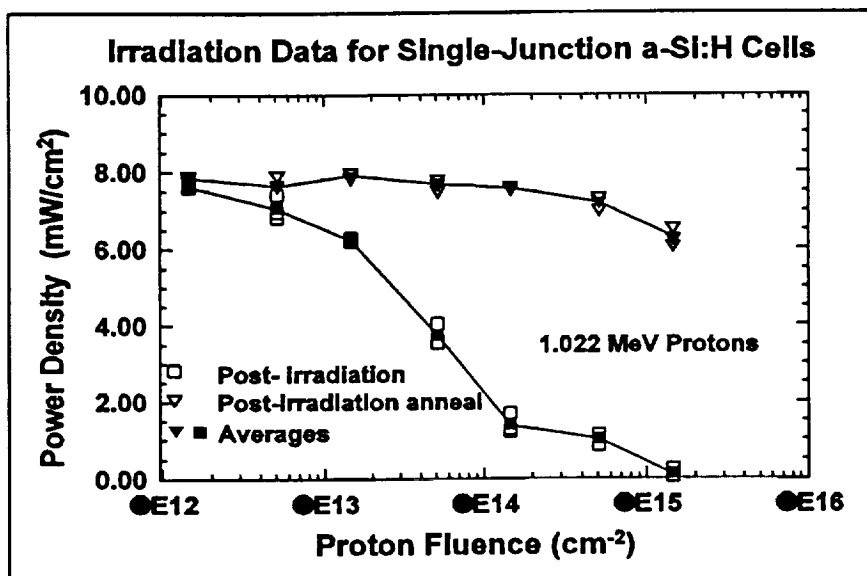

Figure 2: Power densities of twenty-one cells a-Si:H single-junction cells measured after 1.022 MeV proton irradiation and following a post-irradiation anneal at 200 °C for two hours.
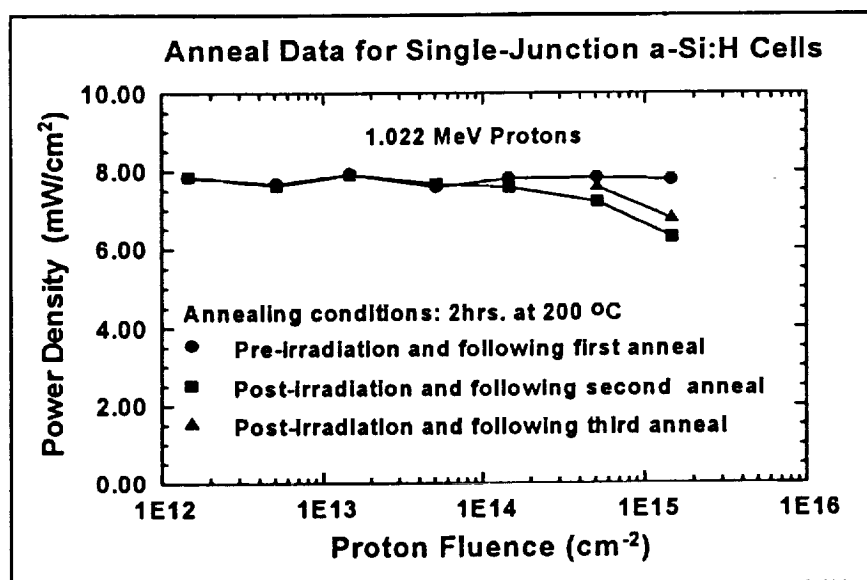

Figure 3: Average power densities following the first pre-irradiation anneal, and the second and third post-irradiation anneals of single-junction cells irradiated with 1.022 MeV protons.

respectively. The details of the time dependence of annealing have been reported in reference 6. In general, the higher the fluence for MeV protons, the longer the annealing time to restore the normalized power density.

The cross-over of the dual and triple-junction curves in Figure 1 at a fluence of 1E14 cm^{-2} is believed to be due the difference in the irradiances of the simulators used to measure the light I-V characteristics of the cells. The dual-junction cells were measured with a simulator which was optimized to match an AM1.5 global spectrum. The triple-junction cells were measured with our simulator which is an ORC model SS1000. The spectral irradiance of the ORC simulator contains xenon lines above 800 nm and is deficient in the red. The thicknesses of the i-layers in the triple-junction cells were matched to an AM1.5 global spectrum. The mismatch between the ORC simulator spectrum and the triple-junction cells probably resulted in the bottom junction limiting the cell current. We have modified the ORC simulator by adding a cold mirror and tungsten-halogen lamp (ref. 7). We plan to repeat the triple-junction measurements with the dual-source simulator to determine the reason for the cross-over of the dual-and triple-junction curves in Figure 1.

The investigations summarized in Figure 1 must be extended to a range of proton and electron energies. It is our expectation that the measurements will provide the basic parameters for the development of a predictive model for determining the EOL performance of cells fabricated from hydrogenated amorphous silicon based alloys in a variety of space environments. We plan to apply the techniques learned from our investigations with hydrogenated amorphous silicon based alloys to other thin-film solar cells of interest for space-power generation.

PARAMETRIC FITTING MODEL

The first step in developing a predictive model for EOL performance is the determination of parameters from measurements which can be related to basic material properties of solar cells. We have elected to develop a parametric fitting model to characterize current mechanisms in single-junction cells. Single-junction cells were chosen because triple-junction cells are far more complex in structure. Dark I-V characteristics were selected for the initial modelling investigations because they showed the largest changes in parameters with 1.0 MeV proton irradiation.

Determination of solar cell parameters from measured dark I-V characteristics requires curve fitting a parametric model to measured dark I-V characteristics. The objective of curve fitting is to minimize the differences between measured and calculated dark I-V characteristics. The parametric model which we developed includes current mechanisms which are characterized by a sum of analytical functions with parameters. The parameters in the analytical functions are referred to as fitting parameters; they are varied to fit a calculated I-V characteristic to a measured dark I-V characteristic. The model was used for analysis of dark I-V characteristics in the forward-bias region. The parametric model used for curve fitting is:

$$I = I_o \left[\exp\left(\frac{q(V-IxR_{se})}{nkT}\right) - 1 \right] + \frac{(V-IxR_{se})}{R_{sh}} + \alpha(V-IxR_{se})^m$$

3

where I_o = thermal generation current R_{se} = series resistance
V = applied bias voltage R_{sh} = shunt resistance
q = electronic charge   α,m = constants
n = quality factor   k = Boltzmann constant
T = temperature

The parameters in the equation may be related to physical mechanisms which are responsible for carrier transport in a solar cell. Each mechanism requires one or two fitting parameters. The four mechanisms used in the forward-bias region of the dark I-V curve-fitting investigations are:

1. Injection current represented by the first term in the equation. The first term is the result of the simple diode equation. The model does not differentiate between injection and recombination current. It may be inappropriate to apply this expression to a p-i-n device, but it is useful for characterizing irradiation effects. The injection current parameters are I_o and n.

2. Shunt current represented by the parameter R_{sh} in the second term.

3. Electric field and depletion effects in the intrinsic layer represented by the parameters α and m in the last term.

4. Series resistance represented by R_{se} in all three terms.

The results of curve fitting the dark I-V characteristic of a single junction cell in the forward-bias region is shown in Figure 4; the cell has a 500 nm thick intrinsic layer. The dark I-V characteristic was measured following the first two-hour anneal at 200 °C following receipt of the cell from the fabricator. Curve fitting was carried out using Matlab software which employs a Nelder-Meade simplex search subroutine. The measured I-V values

Parametric Fit to a Single-Junction Cell I-V Characteristic

$I_o = 1.5E\text{-}11$ A $R_s = 27\Omega$ series
n = 1.74   α = 1.5 E-5
$R_{sh} = 800$ KΩ   m = 2.5

shunt

depletion

injection

■ Measured
△ Calculated

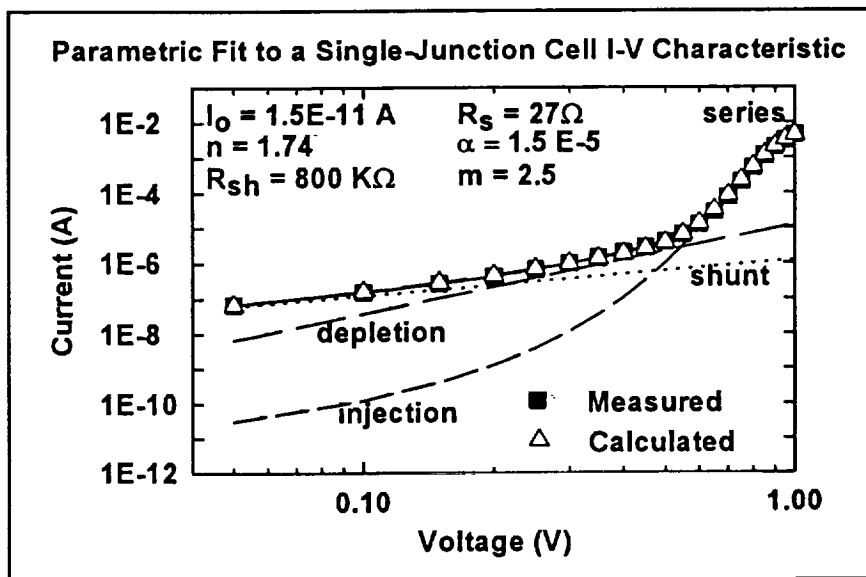Current (A): 1E-2, 1E-4, 1E-6, 1E-8, 1E-10, 1E-12

Voltage (V): 0.10   1.00

Figure 4: Typical curve fitting results for a single-junction cell showing the contributions of each of the four current mechanisms in a dark I-V characteristic.

and calculated results are represented by filled squares and open triangles, respectively. The symbols for the calculated values are plotted over the measured values, and because

the fit is good, the filled squares are barely discernable. The contributions of each of the four current mechanisms are plotted and identified with labels in Figure 4. The voltage ranges where the four mechanisms dominate in a major way are shown in Table I.

Table I

Voltage Range (V)	Dominant Mechanism	Corresponding Parameters
0-0.2	shunt	R_{sh}
0.20-0.60	depletion	a,m
0.60-1.00	injection	I_o n
near 1.00	series	R_{se}

A parametric study was carried out using seven single-junction cells with 500 nm i-layers. The cells were annealed for two hours at 200 °C following delivery. I_o was in the 1.5E-11 to 2.0 E-11 A range. The quality factor, n, ranged from 1.73 to 1.77. The series resistance, R_{se} varied from 25 to 37 Ω. The parameter, a, ranged from 1.0 to 1.4 E-5 A/V$^{2.5}$ m remained constant at 2.5. Agreement between the parametric model and measured I-V characteristic for the cells was <4% for the shunt and injection regions, and <8% in the depletion region.

The dark I-V characteristics of a-Si:H single-junction cells have been investigated to determine the effects of proton irradiation on cell behavior; the cells had 500 nm thick intrinsic layers. The parametric model was used to quantify changes in dark I-V characteristics resulting from 1.00 MeV proton irradiation. The cells studied were irradiated with 1.00 MeV proton fluences between 1.46E12 and 1.46E15 cm^{-2} There were twenty-one cells in the group, with three cells irradiated at each of the fluences. One cell was chosen for the parametric study from each of the fluences studied; the cell with lowest shunt current in the group of three cells was selected in order to determine fitting parameters with the best accuracy. Figure 5
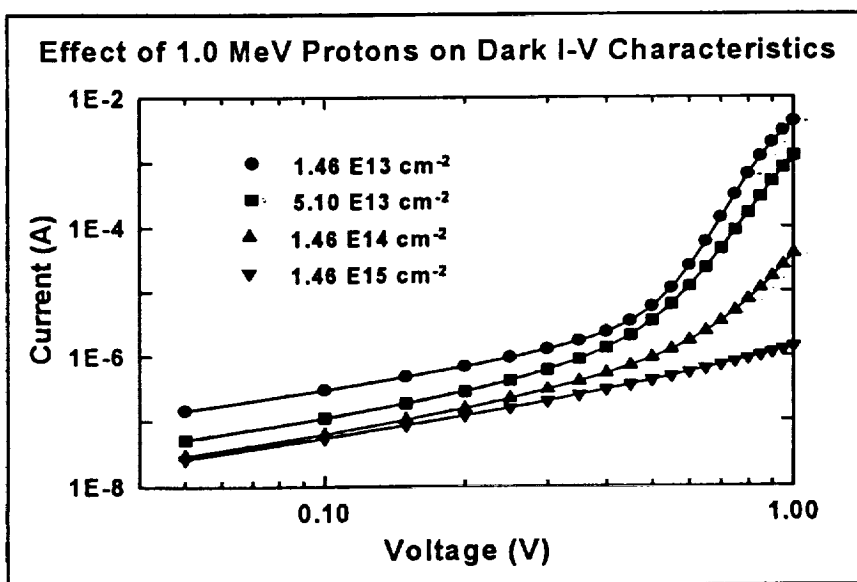

Effect of 1.0 MeV Protons on Dark I-V Characteristics

- 1.46 E13 cm^{-2}
- 5.10 E13 cm^{-2}
- 1.46 E14 cm^{-2}
- 1.46 E15 cm^{-2}

Current (A) / Voltage (V)

Figure 5: Plot of measured dark I-V characteristics for single-junction cells irradiated at various proton fluences.

shows the effect of 1.00 MeV proton fluences on the measured dark I-V characteristics for four of the seven fluences investigated. The figure shows increasing proton fluences result in lower currents in the 0.60 to 1.00 V range, the range associated with the injection current; it also shows the current in the 0.050 to 0.20 V range is lower for higher fluences; the current in this range is due primarily to the shunt current mechanism.

Significant changes occurred in the thermal generation current density, J_O with irradiation and annealing. Figure 6 shows J_O following anneal 1, the first anneal after receiving the cells and pre-irradiation. J_O following anneal 1 is shown by open circles positioned on the graph at fluences the cells were to be irradiated. Following irradiation J_O increased by a factor of two for a fluence of $1.5E12$ cm^{-2} and more than four orders of magnitude for a fluence of $1.5E15$ cm^{-2} After annealing for two hours at 200 °C, labeled anneal 2 on Figure 6, J_o was restored to near pre-irradiated values for fluences less than $1.5E14$ cm $^{-2}$. A third anneal further restored
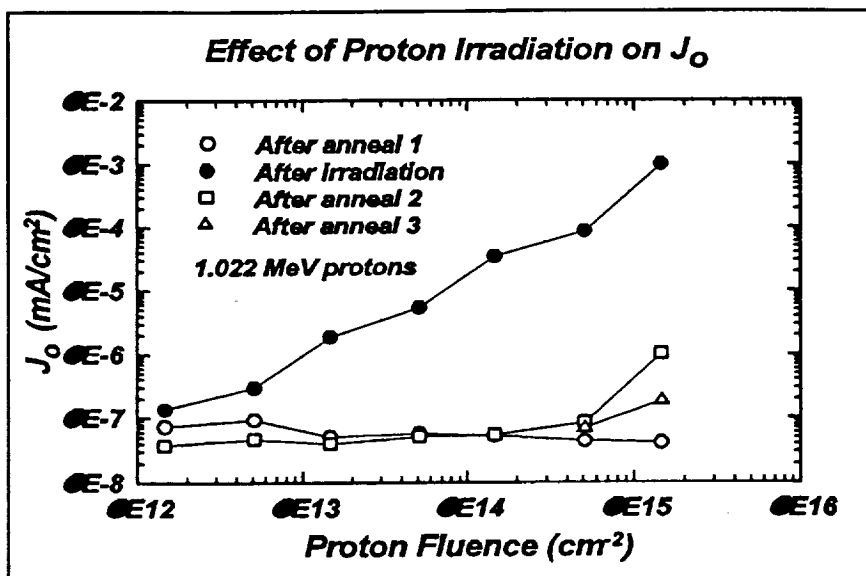

Figure 6: Plot showing the effect of proton irradiation at various fluences and subsequent annealing on reverse saturation current density, J_O obtained from parametric fitting.

J_O for the two highly irradiated cells. J_O is much more sensitive to irradiation than power density. Figure 2 shows only a few percent change in power density at a fluence of $1.5E12$ cm^{-2} while Figure 6 shows a factor of two change in J_O

Changes in quality factor, n, were also observed. Figure 7 is a graph of fitted n values for pre-irradiation, post- irradiation and post-annealing conditions. For the same fluence range, n increased from 1.84 to 23.9 with irradiation. Subsequent anneals restored n to near pre-irradiated values as shown by the overlaid plots for these data; the open symbols essentially coincide for anneals one, two and three. These results are consistent with the literature which shows J_O and n increase as the quality of device material degrades; degradation in the material is believed to be due to an increase in defect density.

R_{se} does not appear to be significantly influenced by irradiation. One exception was noted. R_{se} for one cell increased from 28 to 53 Ω following irradiation; it was restored to 32 Ω with annealing. The reasons for the large change in R_{se} for this cell are not understood. It is important to note that as the injection current decreases with increasing fluence, R_{se} becomes less of a factor in the I-V characteristic and parametric fitting of R_{se} becomes more difficult.

The depletion current fitting parameters, a & m, behave differently with fluence. a is

6

influenced by irradiation, while m does not appear to change with irradiation. α decreases from its annealed pre-irradiated value, approximately 1E-5 $A/V^{2.5}$ to about 7E-7 $A/V^{2.5}$ with the largest fluence. It recovers to the 3E-6 to 5E-6 $A/V^{2.5}$ range with annealing. We think it is significant that α does not recover to the annealed pre-irradiated value. m appears to remain constant at 2.5 with irradiation and annealing.
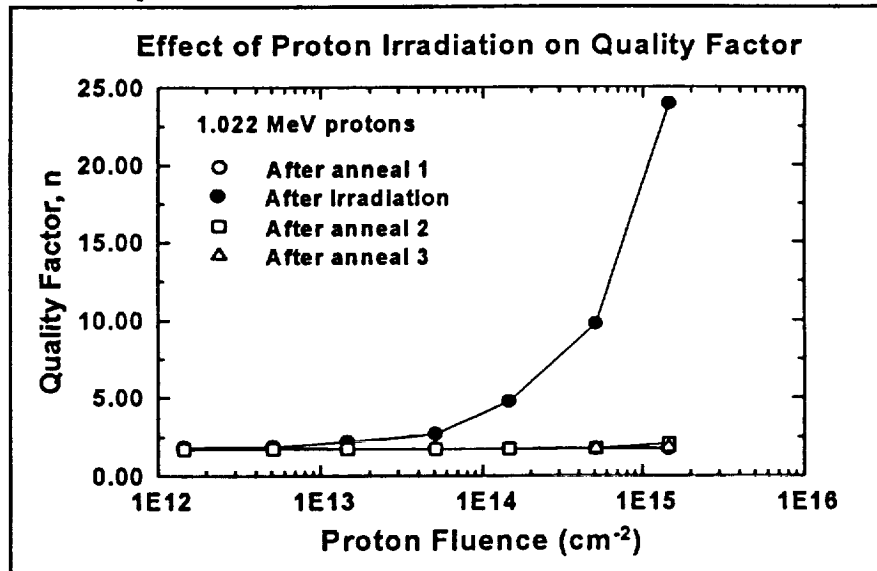

Figure 7: Plot showing the effect of proton irradiation at various fluences and subsequent annealing on quality factor, n, obtained from parametric fitting.

R_{sh} of the cells appears to increase with irradiation and decrease with annealing. Pre-irradiation R_{sh} values range between about 300 and 800 kΩ, and increase to about 2000 kΩ with irradiation. R_{sh} decreases with annealing to values which range between 300 to 900 kΩ. R_{sh} exhibits a switching behavior. R_{sh} of the twenty-one irradiated cells was determined under three conditions: pre-irradiation, post-irradiation, and post-irradiation annealing. The behavior of R_{sh} from the analysis of the cells was similar to above results. R_{sh} was calculated using the current at a forward bias of 0.050 V; the procedure assumes R_{sh} dominates the current. The average R_{sh} prior to irradiation was 417 kΩ. Of the twenty-one cells, sixteen exhibited an increase in R_{sh} after 1.00 MeV proton irradiation. Cells irradiated with the same fluences did not exhibit the same changes in R_{sh} and the reasons for this are not understood. The average R_{sh} increased to approximately 590 kΩ following irradiation. After annealing, seventeen of the twenty-one cells exhibited a decrease in R_{sh} The average R_{sh} following post-irradiation annealing was about 300 kΩ. The analysis of twenty-one irradiated cells confirms the trend that R_{sh} is increased by irradiation and decreases with post-irradiation annealing.

We plan to pursue device simulation studies in an effort to explain the role of irradiation, in terms of fundamental material properties, on the parameters resulting from the fitting model.

INSTABILITY STUDIES

Triple-tandem cells cut from a module had fill-factors ranging from 0.37 to 0.68 under as-received or virgin conditions. Figure 8 shows light I-V characteristics for a cell under two conditions; the filled circles are for virgin conditions and result in a fill-factor of 0.37. The virgin cell is characteristic of one of the poorer as-received cells. Note the current has

an unexpected structure between 1.50 and 2.00 V; the structure is concave down instead of concave up as would be expected. Following a two hour anneal at 200 °C, a light I-V measurement produced the open squares in Figure 8; the corresponding fill-factor is 0.66. After annealing the cell, the light I-V characteristic was similar to one of the better as-received cells. The fabricator of the triple tandem cells indicated
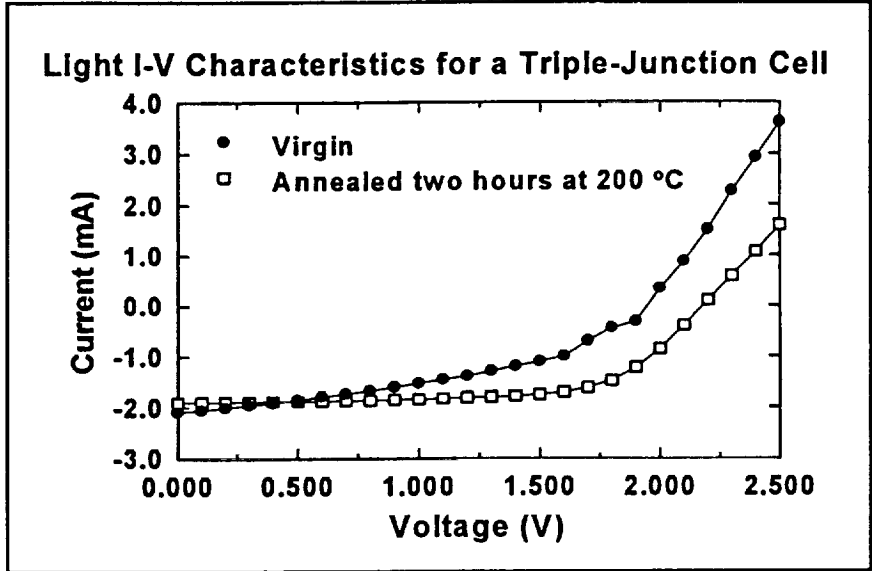

Figure 8: Light I-V characteristic for a triple-junction cell measured under virgin and annealed conditions.

the module was annealed for one hour in air at 100 °C following fabrication; the annealing procedure is employed by the fabricator as one of the steps in the fabrication of modules.

It is difficult to investigate current mechanisms in triple-junction cells because of their complex structure. For this reason, single-junction cells were investigated in an effort to determine if the behavior observed in Figure 8 is also characteristic of single-junction cells. Figure 9 shows light I-V measurements for a single-junction cell under light soaked and annealed conditions. The filled squares correspond to light I-V measurements for the cell annealed at 200 °C for two hours. I-V measurements following 32 hours of room temperature light soaking are represented by open circles. Annealing the cell following light soaking resulted in I-V measurements which are the same as before annealing. A comparison of Figures 8 and 9 shows there is similar structure in the light I-V characteristics, suggesting the current mechanisms resulting in the initially poor performance of this particular triple-junction cell may be elucidated
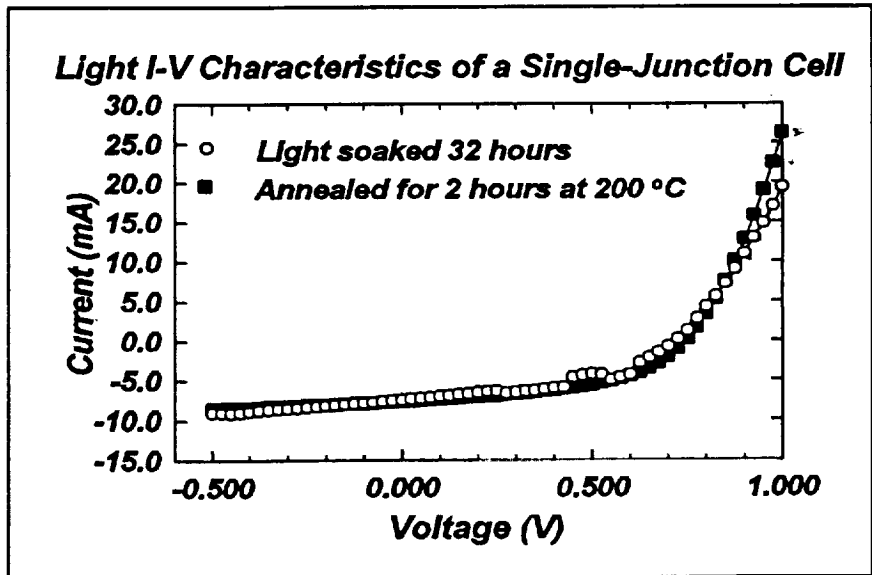

Figure 9: Light I-V characteristics of a single-junction cell under light soaked and annealed conditions.

8

with investigations of single-junction cells.

The effect of light soaking on the forward-bias dark I-V characteristic for a single-junction cell is shown in Figure 10 by open circles. The cell exhibits a switching effect in the region of the I-V characteristic where shunt current is the dominant current mechanism. The switching effect has been observed in several cells; it occurs under both forward and reverse-bias conditions. An analysis of several cells shows the switching effect increases in frequency with light and forward-bias voltage soaking. It decreases with annealing and reverse-bias voltage soaking. The filled squares in Figure 10 represent a dark I-V

Dark I-V Characteristics of a Single-Junction Cell

○ *Light soaked 32 hours*
■ *Reverse biased at -2.00 V*

Figure 10: Dark I-V characteristics of a single-junction cell following light soaking and reverse-bias voltage soaking.

characteristic measured following the application of a -2.00 V reverse-bias voltage for five minutes; this characteristic also corresponds to annealing at 200 °C for two hours. The figure clearly demonstrates the role the history of the cell plays in I-V characteristics.
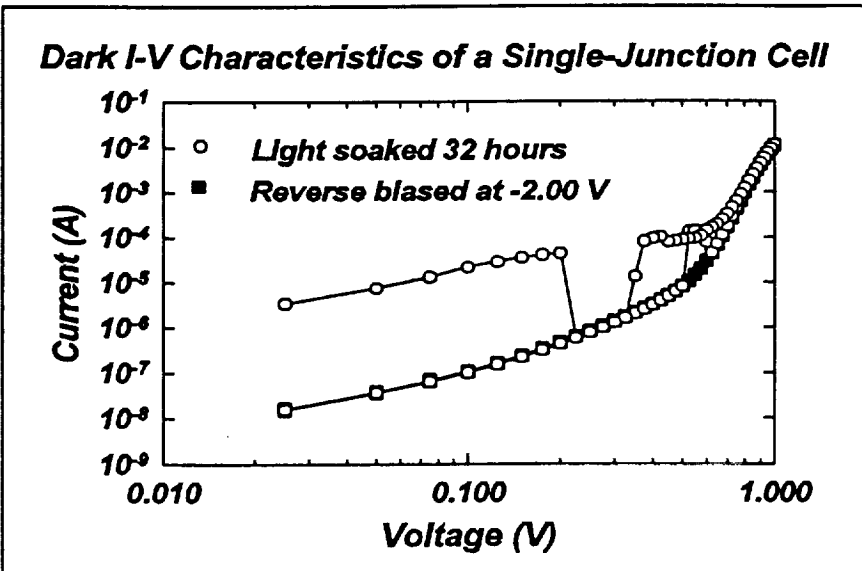
Close inspection of dark I-V characteristics suggested the characteristics exhibited a time dependence. The role of time was investigated by including a delay time in the computer program. Measurements were taken with one and ten minute delays between the source-bias voltage steps. Time-dependent switching was observed in the reverse-bias voltage region of the dark I-V characteristics where the current switched from shunt dominated to a current mechanism with a slope between two and two and one-half. Switching occurred at lower reverse-bias voltages as the delay time was increased, and the reverse-bias current was higher; the current mechanism is not understood. I-V characteristics exhibited another time dependence; as the voltage was scanned from the reverse-bias to the forward-bias region, the current decreased with increasing delay times. The observation suggests charge stored in a cell during reverse bias contributes to the current in the forward-bias region; however, the mechanism has not yet been fully characterized.

DEVICE SIMULATION

We have carried out device simulations with EPRI AMPS (ref. 8) in order to produce I-V characteristics. The simulated I-V characteristics may be compared with measured characteristics in an effort to determine fundamental material parameters. Changes were made in the material parameters for a simulation in order to produce an I-V

characteristic similar to one obtained by measurement. Simulations were carried out and compared to I-V characteristics measured following irradiation of cells. The comparison provides information on the role of irradiation on fundamental material parameters. An understanding of the role of irradiation on the fundamental material parameters is necessary in order to develop a model for predicting EOL cell performance in a given space radiation environment. The work reported in this section represents our first efforts to use EPRI AMPS simulations to understand the effects of 1.0 MeV proton irradiation on hydrogenated amorphous silicon alloy based solar cells.

EPRI AMPS was used to simulate a PIN device structure using various i-layer thicknesses and sub-band-gap density of state, DOS, functions. Devices were simulated with i-layer thicknesses of 200, 500, and 800 nm; 20 nm thick n^+-layers and p^+-layers were used. Gaussian and U-shaped DOS functions were used in the simulations. Characteristics of devices were simulated with midgap DOS values of 5E15, 5E16, 5E17, and 5E18 cm^{-3} eV^{-1}. The effective DOS at the conduction and valence band edges was 1E19 cm^{-3}. Devices were simulated under thermodynamic equilibrium conditions as well as light and voltage bias conditions. Light and dark I-V's and electric field distributions have been generated in these preliminary simulations.

The electric field is shown in Figure 11 for thermodynamic equilibrium conditions . The figure shows the spatial distribution of the electric field in a p^+-i-n^+ cell for a U-shaped DOS function with minimum DOS values of 5E15, 5E17, and 5E18 cm^{-3} eV^{-1}. For reference purposes, the cell layers are shown at the bottom of Figure 11. The n^+-layer extends from 0 to 20 nm, the i-layer from 20 to 520 nm, and the p^+-layer from 520 to 540 nm. The electric field decreases in the middle of
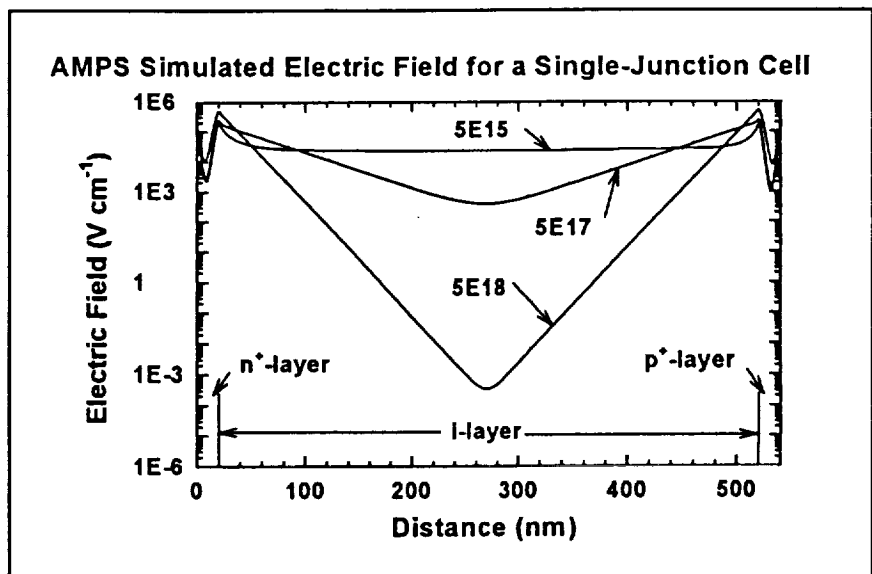

Figure 11: AMPS simulated thermodynamic equilibrium electric field for a 500 nm thick I-layer PIN device with 5E15, 5E17, 5E18 cm^{-3} eV^{-1} midgap DOS.

the i-layer as the DOS is increased. The results suggest the reason for the decrease in cell power density with increasing 1.0 MeV proton fluence is the generation of defects in the i-layer. Defects in the EPRI AMPS model are represented by electron energy states in the sub-band-gap region. The effect of the defects is to trap charge carriers which increases the space-charge density. The increased space charge density in the i-layer reduces the electric field distribution which in turn reduces the collection of carriers. We plan to pursue the EPRI AMPS simulation in order to obtain the fundamental material parameters for the development of a predictive model.

CONCLUSIONS

The effect of 1.0 MeV proton irradiation is to degrade the normalized power density of cells with six different structures by less than a few percent for fluences less than $1E12$ cm^{-2} For fluences above $1E15$ cm^{-2} cell power degrades to less than 10% of the initial power. Reductions in the normalized power density in the $1E12$ through $1E14$ cm^{-2} proton fluence range depends on cell structure. Cells with triple junctions have the best radiation resistance, dual-junction cells are next, and single-junction cells have the lowest radiation resistance. Single-junction cells with a-Si,Ge:H i-layers have better radiation resistance than cells with a-Si:H i-layers. A parametric fitting model was employed to determine the effect on 1.0 MeV proton irradiation on cell parameters. Following irradiation J_o increased by a factor of two for a fluence of $1.5E12$ cm^{-2} and more than four orders of magnitude for a fluence of $1.5E15$ cm^{-2} After annealing for two hours at $200^{\circ}C$, J_o was restored to near pre-irradiated values for fluences greater than $1.5E14$ cm^{-2} A third anneal further restored J_o for the two highly irradiated cells. J_o was found to be more sensitive to irradiation than power density. Changes in the quality factor, n, were also observed with irradiation. The quality factor increased from 1.84 to 23.9 with irradiation; annealing at 200 °C restored n to near pre-irradiated values. The investigations show there is similar structure in the light I-V characteristics of triple and single-junction cells suggesting the current mechanisms resulting in the initially poor performance of a triple-junction cell may be elucidated with investigations of single-junction cells. Investigations of dark I-V characteristics show there is a switching effect in the region of the I-V characteristic where shunt current is the dominant current mechanism. The switching effect has been observed in several cells; it occurs under both forward and reverse-bias conditions. An analysis of several cells shows the switching effect increases in frequency with light and forward-bias voltage soaking; it was observed to decrease with annealing and reverse-bias voltage soaking. Time-dependent switching was observed in the reverse-bias voltage region of the dark I-V characteristics where the current switched from shunt dominated to a current mechanism with a slope between two and two and one-half. Switching occurred at lower reverse-bias voltages as the delay time was increased, and the reverse-bias current was higher; the current mechanism is not understood. Device simulation studies were carried to determine the role of the sub-band-gap density of electron states on the electric field distribution in the p^{+}-i-n^{+} ;layers. The electric field decreased in the middle of the i-layer as the density of states was increased. The results suggest the reason for the decrease in cell power density with increasing 1.0 MeV proton fluence is the generation of defects in the i-layer. The effect of the defects is to trap charge carriers which increases the space-charge density. The increased space charge density in the i-layer reduces the electric field distribution which in turn reduces the collection of carriers.

REFERENCES

1. Geoffrey A. Landis and James R. Woodyard, Radiation Damage in Thin Film Solar Cells, Solar Cells, 1991, Volume 31, page 297.

2. James R. Woodyard, Dependence of 1.0 MeV Proton Radiation Resistance of a-Si:H Alloy Solar Cells on Cell Thickness, Amorphous Silicon Technology-1992, Materials Research Society Symposium Proceedings, Edited by Malcolm J. Thompson, Yosihhiro Hamakawa Peter G. LeComber Arun Madan and Eric Schiff, Volume 258, 1992, page 1151.

3. Kenneth R. Lord II, Michael R. Walters and James R. Woodyard, Investigation of the Radiation Resistance of Triple-Junction A-Si:H Alloy Solar Cells Irradiated with 1.00 MeV Protons, Space Photovoltaic Research and Technology 1992, NASA Conference Publication 3210, page 98.

4. Kenneth R. Lord II, Michael R. Walters and James R. Woodyard, Investigation of Light and Dark Characteristics of a-Si:H Alloy Cells Irradiated with 1.0 MeV Protons, Twenty Third IEEE Photovoltaic Specialists Conference-1993, page 1448.

5. Kenneth R. Lord II, Michael R. Walters and James R. Woodyard, Investigation of Shunt Resistances in Single-Junction a-Si:H Alloy Solar Cells, Amorphous Silicon Technology-1994, Materials Research Society Symposium Proceedings, Edited by Malcolm J. Thompson, Yosihhiro Hamakawa Peter G. LeComber Arun Madan and Eric Schiff, In Press.

6. S. Abdulaziz and J. R. Woodyard, Annealing Characteristics of Amorphous Silicon Solar Cells Irradiated with 1.00 MeV Protons, Eleventh Space Photovoltaic Research and Technology Conference-1991, NASA Conference Publication 3121, 1991, page 43-1.

7. M. Bennettt and R. Podlesny, Two-Source Simulator for Improved Solar Simulation, Twenty-First IEEE Photovoltaic Specialists Conference-1990, page 1438.

8. J. K. Arch, P. J. McElheny, S. J. Fonash, and W. H. Howland. AMPS/1D: A One-Dimensional Device Simulation Program for the Analysis of MicroElectronic and Photonic Structures. Penn State University. November 2, 1990.

Papers Published with NASA Support

Radiation Resistance Studies of Amorphous Silicon Films, James R. Woodyard and J. Scott Payson, Space Photovoltaic Research and Technology Conference-1988, NASA Conference Publication 3030, page 339.

Radiation Resistance Studies of Amorphous Silicon Films, J. Scott Payson and James R. Woodyard, Proceedings of the Twentieth IEEE Photovoltaic Specialists Conference, 1988, page 990.

Radiation Effects on the Optical and Transport Properties of Amorphous Silicon, J. Scott Payson, Yang Li and James R. Woodyard, Amorphous Silicon Technology-1989, Materials Research Society Symposia Proceedings, Edited by D. Adler, A. Madan, M. J. Thompson, P. C. Taylor, Y. Hamakawa and P. G. LeComber, 1989, Volume 149, page 321.

Annealing Characteristics of Irradiated Hydrogenated Amorphous Silicon Solar Cells, J. S. Payson, S. Abdulaziz, Y. Li and J. R. Woodyard, Tenth Space Photovoltaic Research and Technology Conference-1989, NASA Conference Publication 3107, 1990, page 389.

1.00 MeV Proton Induced Defects in a-Si:H Thin Films and Solar Cells, Materials Research Society, J. Scott Payson, Salman Abdulaziz, Yang Li and James R. Woodyard, Amorphous Silicon Technology-1990, Materials Research Society Symposium Proceedings, Edited by P. C. Taylor, M. J. Thompson, P. G. LeComber, Y. Hamakawa and A. Madan, 1990, Volume 192, page 63.

Annealing Characteristics of Amorphous Silicon Films and Solar Cells Irradiated with 1.00 MeV Protons, Salman Abdulaziz, J. Scott Payson, Yang Li and James R. Woodyard, 21st IEEE Photovoltaic Specialists Conference Proceedings, 1990, page 1510.

Annealing Characteristics of Amorphous Silicon Solar Cells Irradiated with 1.00 MeV Protons, S. Abdulaziz and J. R. Woodyard, Eleventh Space Photovoltaic Research and Technology Conference-1991, NASA Conference Publication 3121, 1991, page 43-1.

Thin Film Development Workshop Report, J. R. Woodyard, Eleventh Space Photovoltaic Research and Technology Conference-1991, NASA Conference Publication 3121, 1991, page 48-1.

Annealing Studies of Damage Produced by 1.00 MeV Proton Irradiation of a-Si:H and a-Si, Ge:H Solar Cells, Materials Research Society, Salman Abdulaziz and James R. Woodyard, Amorphous Silicon Technology-1991, Materials Research Society Symposium Proceedings, Edited by P. C. Taylor, M. J. Thompson, P. G. LeComber, Y. Hamakawa and A. Madan, 1991, Volume 219, page 463.

Investigation of Solar Cell Thickness on MeV Proton Radiation Resistance, Salman Abdulaziz and James R. Woodyard, 22st IEEE Photovoltaic Specialists Conference Proceedings, 1991, page 1248.

Radiation Damage in Thin Film Solar Cells, James R. Woodyard and Geoffrey A. Landis, Solar Cells, 1991, Volume 31, page 297 (Invited Review Article).

Dependence of 1.0 MeV Proton Radiation Resistance of a-Si:H Alloy Solar Cells on Cell Thickness, James R. Woodyard, Amorphous Silicon Technology-1992, Materials Research Society Symposium Proceedings, Edited by Malcolm J. Thompson, Yosihhiro Hamakawa, Peter G. LeComber, Arun Madan and Eric Schiff, 1992, Volume 258, page 1151.

Investigation of the Radiation Resistance of Triple-Junction A-Si:H Alloy Solar Cells Irradiated with 1.00 MeV Protons, Kenneth R. Lord II, Michael R. Walters and James R. Woodyard, Space Photovoltaic Research and Technology 1992, NASA Conference Publication 3210, page 98.

Investigation of Light and Dark Characteristics of a-Si:H Alloy Cells Irradiated with 1.0 MeV Protons, Kenneth R. Lord II, Michael R. Walters and James R. Woodyard, Twenty Third IEEE Photovoltaic Specialists Conference-1993, page 1448.

Investigation of Shunt Resistances in Single-Junction a-Si:H Alloy Solar Cells, Kenneth R. Lord II, Michael R. Walters and James R. Woodyard, Amorphous Silicon Technology-1994, Materials Research Society Symposium Proceedings, Edited by Eric A. Schiff, Michael Hack, Arun Madan, Martin Powell and Akihisa Matsuda, 1994, Volume 336, page 729.

Investigation of the Stability and 1.0 MeV Proton Radiation Resistance of Commercially Produced Hydrogenated Amorphous Silicon Alloy Solar Cells, Kenneth R. Lord II, Michael R. Walters and James R. Woodyard, Proceedings of the XIII Space Photovoltaic Research and Technology Conference 1994, NASA Conference Publication 3278, page 187.

Investigation of Current Mechanisms in a-Si:H Alloy Cells, Kenneth R. Lord II, Fazal UrRahman Syed, Michael R. Walters and James R. Woodyard, First World Conference on Photovoltaic Energy Conversion, Twenty Fourth IEEE Photovoltaic Specialists Conference-1994, page 993.

Laboratory Instrumentation and Techniques for Characterizing Multi-Junction Solar Cells, James R. Woodyard, Proceedings of the XIV Space Photovoltaic Research and Technology Conference 1995, NASA Conference Publication 10180, page 158.

INVENTIONS STATEMENT

There were no inventions during the period of NASA support.